Tissue Eng Regen Med (2018) 15(6):761–769
https://doi.org/10.1007/s13770-018-0144-8

Online ISSN 2212-5469
Print ISSN 1738-2696

ORIGINAL ARTICLE

Development and Evaluation of Hyaluronic Acid-Based Hybrid Bio-Ink for Tissue Regeneration

Jaeyeon Lee[1] · Se-Hwan Lee[2] · Byung Soo Kim[3] · Young-Sam Cho[2] · Yongdoo Park[1]

Received: 30 March 2018 / Revised: 17 June 2018 / Accepted: 10 July 2018 / Published online: 21 September 2018

Abstract

BACKGROUND: Bioprinting has recently appeared as a powerful tool for building complex tissue and organ structures. However, the application of bioprinting to regenerative medicine has limitations, due to the restricted choices of bio-ink for cytocompatible cell encapsulation and the integrity of the fabricated structures.

METHODS: In this study, we developed hybrid bio-inks based on acrylated hyaluronic acid (HA) for immobilizing bio-active peptides and tyramine-conjugated hyaluronic acids for fast gelation.

RESULTS: Conventional acrylated HA-based hydrogels have a gelation time of more than 30 min, whereas hybrid bio-ink has been rapidly gelated within 200 s. Fibroblast cells cultured in this hybrid bio-ink up to 7 days showed $> 90\%$ viability. As a guidance cue for stem cell differentiation, we immobilized four different bio-active peptides: BMP-7-derived peptides (BMP-7D) and osteopontin for osteogenesis, and substance-P (SP) and Ac-SDKP (SDKP) for angiogenesis. Mesenchymal stem cells cultured in these hybrid bio-inks showed the highest angiogenic and osteogenic activity cultured in bio-ink immobilized with a SP or BMP-7D peptide. This bio-ink was loaded in a three-dimensional (3D) bioprinting device showing reproducible printing features.

CONCLUSION: We have developed bio-inks that combine biochemical and mechanical cues. Biochemical cues were able to regulate differentiation of cells, and mechanical cues enabled printing structuring. This multi-functional bio-ink can be used for complex tissue engineering and regenerative medicine.

Keywords Bio-ink · Bioprinting · Hyaluronic acid · Hydrogel · Tissue engineering

1 Introduction

Bio-printing for complex tissue regeneration is one of the leading issues in tissue engineering and regenerative medicine [1–4]. Developing highly organized three-dimensional (3D) scaffolds for complex tissue regeneration requires a precisely controlled 3D printing system. In particular, the development of novel materials called 'bio-ink' for building 3D structures is one of the challenging issues in bio-printing [5–8]. For the ideal bio-ink, materials have to be biomimetic to characteristics of the microenvironment of tissues, have mechanical integrity for maintaining 3D structures and provide instructive guidance for tissue regeneration [9, 10].

Electronic supplementary material The online version of this article (https://doi.org/10.1007/s13770-018-0144-8) contains supplementary material, which is available to authorized users.

✉ Yongdoo Park
ydpark@kumc.or.kr

[1] Department of Biomedical Engineering, College of Medicine, Korea University, 73 Inchon-ro, Seongbuk-gu, Seoul 02841, Republic of Korea

[2] Department of Mechanical Design Engineering, College of Engineering, Wonkwang University, 460 Iksandae-ro, Iksan, Jeonbuk 54538, Republic of Korea

[3] Department of Internal Medicine, Korea University Medical Center, 73 Inchon-ro, Seongbuk-gu, Seoul 02841, Republic of Korea

For maintaining 3D structures, gelation kinetics is challenging. Fast gelation of bio-ink guarantees layer-by-layer deposition for 3D structure fabrication. Li et al. combined two DNA-based hydrogels as bio-inks for a fast gelation. The mixing of a polypeptide-DNA conjugate and a complementary DNA linker led to rapid hydrogel formation, owing to DNA hybridization. Anterior pituitary cells (AtT-20) were found to have normal viability in a polupeptide-DNA-hydrogel [11]. A requirement for an ideal bio-ink is mechanical integrity of the supporting 3D structure. Rutz et al. developed degradable and tunable bio-inks based on polyethylene glycol (PEG) with two reactive groups at the end of the polymer. Culturing human umbilical vein endothelial cells (HUVEC) and hMSC in this bio-ink demonstrated the bio-ink's modulated degradability and tissue formation [12].

Incorporating biological functions into scaffolds is another challenge when developing bio-inks. Biological functions in the scaffolds are achieved by making composite or hybrid scaffolds with the components of extracellular matrix proteins. Duan et al. [13] fabricated a human trileaflet heart valve conduit based on hyaluronic acid and gelatin gels seeded with human aortic valve interstitial cells, which showed higher cellular survival rates and remodeling activity after 7 days in culture. A composite bio-ink with gelatin and alginate showed similar results [14]. Pati et al. developed a decellularized extracellular matrix-based bio-ink for guiding stem cell fates [15]. Das et al. [16] fabricated a silk fibrin-gelatin bio-ink with a combination of enzymatic and physical crosslinking reactions for guiding cell fates.

For specific guidance of cell behaviors in bio-inks, growth factors or peptides have been used, either immobilized or incorporated in the hydrogels. Complex biological processes in MSCs are elicited by incorporating small-molecule chemical functional groups into the hydrogel [17]. Immobilization of angiogenic peptides, such as ac-SDKP, into hydrogels improved the regeneration of infarcted hearts by stimulating angiogenesis [18]. Incorporation of BMPs into hydrogels also increased bone regeneration [19]. Composite scaffolds with alginate and poly(γ-glutamic acid) (γ-PGA) with neuron growth factor (NGF) induced differentiation of iPS cells into neurons [20].

In this study, we developed functional hybrid bio-ink with fast gelation time and biological function based on hyaluronic acid (HA) which is the main component of ECM scaffold. For fast gelation, tyramine was conjugated to amine group of hyaluronic acids for enzymatic crosslinking reaction. Also, for application to complex tissue such as bone, angiogenic peptides such as substance P (SP) and Ac-SDKP (SDKP) and osteogenic peptides such as BMP-7-derived peptides (BMP-7D) and osteopontin (OPN) were immobilized on acrylated HA. We evaluated the mechanical properties, cell viability and the differentiation rate of hMSC cells according to these four peptide-immobilized hybrid inks.

2 Materials and methods

2.1 Materials

1-ethyl-3-(3 dimethylaminopropyl) carbodimide (EDC), adipic acid dihydrazide (ADH), tyramine hydrochloride (Tyr·HCl), *N*-hydroxysuccinimide (NHS), and triethanolamine (TEA) were acquired from Sigma-Aldrich (St. Louis, MO). 1-hydroxybenzotriazole hydrate (HOBT) was purchased from Fluka Chemical (Fluka Chemical AG, Buchs, Switzerland). *N*-acryloxysuccinimide (NAS) was purchased from Polyscience (Warrington, PA, USA). Sodium hyaluronate (MW: 200 kDa) was purchased from Lifecore Biomedical Co. (Chaska, MN, USA) Substance P peptide (SP: RPKPQQFFGLMC), Ac-SDKP peptide (SDKP: Ac-SDKPDGPQGIWGQC), BMP-7-derived peptide (BMP-7D: GQGFSYPYKAVFSTQC), Osteopontin peptide (OPN: PSKSNESHDHMDDMDDC) and MMP-sensitive peptide (MMPs: GCRDGPQGIWGQDRCG) were synthesized by Anygen (GwangJu, Korea). HRP was purchased from Wako Pure Chemical Industry (Tokyo, Japan). H_2O_2 was purchased from Daejung Chemicals and Materials (Siheung, Korea). Fetal bovine serum (FBS), penicillin/streptomycin, trypsin, low-glucose Dulbecco's modified Eagle's medium (DMEM) and phosphate buffered saline (PBS, pH 7.4) were purchased from GIBCO BRL (Grand Island, NY, USA).

2.2 Preparation of hybrid hydrogel

Hyaluronic acid derivatives (acrylated HA and tyramine-conjugated HA) were synthesized as per previous studies [19, 21]. Acrylated HA-ac (200 kDa, 3 wt%) was dissolved using TEA buffer. Peptides (SP, SDKP, BMP-7D and OPN) were immobilized on acrylated HA-ac at the molar ratio of 20% of acryl groups of the HA. MMP-sensitive peptide was dissolved in a 0.3 M TEA buffer and then added to the acrylated HA solution with the same molar ratio of 80% acryl and thiol groups (HA-ac solution). Lyophilized HA–Tyr was dissolved in phosphate buffered saline (PBS) at a concentration of 3 wt%. Then, HRP and H_2O_2 were added to a 3 wt% HA-tyr solution. For gelation, HA-ac solution was mixed with HA-tyr solution at a 9:1 ratio.

2.3 Rheological properties of hybrid hydrogels

Rheological measurements of the hybrid hydrogel formation were performed with rheometer DHR-1 (TA Instruments Ltd., DE, USA). Five samples were evaluated, (A) control group (no peptides), (B) SP, (C) SDKP, (D) BMP-7D, and (E) OPN. The mixtures were carried out in 1 ml solution, on a sandblast parallel plate (diameter 15 mm) under the following conditions: gelation was monitored for 15 min by observing the viscosity, and elastic modulus measurements were taken at 37 °C in the dynamic oscillatory mode with a constant deformation of 1% and frequency of 1 Hz.

2.4 Cell preparation and culture

In this experiment, fibriblast cells (L929) purchased from Thermo Fisher (Waltham, MA, USA) were used. The media was replaced every 2–3 days in DMEM supplements containing 10% FBS and 1% penicillin/streptomycin. Human mesenchymal stem cells (hMSCs) were obtained from Lonza (Basel, Switzerland) and maintained in MSCGM medium. All cells were cultured at 37 °C in humidified 5% CO_2 incubator.

2.5 *In vitro* 3D cultures in hybrid hydrogel and viability evaluation

Fibroblast cells were cultured in a T-75 cell culture plate, and adherent cells were isolated by trypsin. The resulting Cell suspension was mixed with a hybrid hydrogel solution with peptides (1×10^6 cells/100 μl gel). Five different peptides groups were used: (A) control group (no peptides), (B) SP, (C) SDKP, (D) BMP-7D, and (E) OPN. The volume of the construct was made to equal 25 ml (n = 4 for each group). The samples were crosslinked for 10 min at 37 °C. The cell-containing hydrogels were cultured in DMEM supplemented with 10% FBS and 1% penicillin/streptomycin for 7 days (5%, CO_2, 37 °C). After 7 days, the viability was measured by the LIVE/DEAD Viability/Cytotoxicity Assay Kit (Molecular Probes, Eugene, OR, USA). Live and dead cells were examined under fluorescence microscopy.

2.6 Quantitative real-time PCR

Total RNA was extracted from the 3D cultures of hMSCs in hybrid hydrogels using Trizol reagent (Invitrogen-Life Technologies, Carlsbad, CA, USA) following the manufacturer's instructions. mRNA expression of von Willebrand factor (vWF, F: CCA GCT TCT GAA GAG CAC; R: GTA CAG CAC CAT TCC CTC CT), α smooth muscle actin (α-SMA, F: CCT ATC CCC GGG ACT; R: ACC CAG TGC TGT CCT CTT CT), Runt-related transcription factor 2 (RUNX2, F: TCT GGC CTT CCA CTC TCA GT; R:GAC TGG CGG GGT GTA AGT AA) and Alkaline phosphatase(ALP, F: AAC ACC ACC CAG GGG AAC; R: GGT CAC AAT GCC CAC AGA TT) was quantified using semi-quantitative reverse transcriptase polymerase chain reactions (qRT-PCR; TAKARA, Shiga, Japan). RNA was reverse transcribed to obtain cDNA using the SYBR Green Premix EX Taq II kit (Takara akara bio inc, Shiga, Japan). Relative quantification of mRNA levels was performed using the Applied Biosystems 7500 Real-Time PCR system (Applied Biosystems, Foster City, CA, USA), which directly monitors the fluorescent signal. The level of gene expression was calculated by comparing the cycle threshold (Ct) value of the β-actin gene (F: ATT GGC AAT GAG CGG TTC; R: GGA TGC CAC AGG ACT CCA T) with the mRNA of interest.

2.7 Fabrication of scaffolds using a 3D printer

A mesh-type hydrogel scaffold was fabricated by a lab-made 3D printer. The 3D printer with compact size was able to fabricate the 3D hydrogel scaffold by dispensing bio-ink material in the clean-bench. The 3D printer has *x*, *y*, *z*, and comparison of mechanical properties-axis. As shown in Fig. 1, the *x* and *y*-axis linear actuators are used for two-dimensional patterning of 3D matrix, and *z*-axis linear actuator was used to control the movement of the syringe pump head in height direction. Additionally, a *A*-axis linear actuator in the syringe pump head was used to control the extrude velocity of a syringe. A 250-μl Hamilton syringe was used to extrude bio-ink material. To investigate motion control parameters near ideal conditions, the printing head pathway was generated by in-house code software. It can easily control the width of the printed strand, the distance between printed strands, and pattern dimensions. A cell-encapsulated hybrid bio-ink scaffold having a 3D grid pattern was fabricated using a needle with an inner diameter of 150 μm. The width (*W*) and length (*L*) were both 5 mm at the fabricated simple-grid scaffold. It was designed to have 1 layers. The extrude velocity and feed rate of the syringe pump head are 0.17 μl/s and 1.30 mm/s, respectively.

2.8 Statistical analysis

All the data are reported as mean ± standard deviation (SD). Comparisons between the two groups were carried out using the Student *t* test. A p value < 0.05 was considered statistically significant.

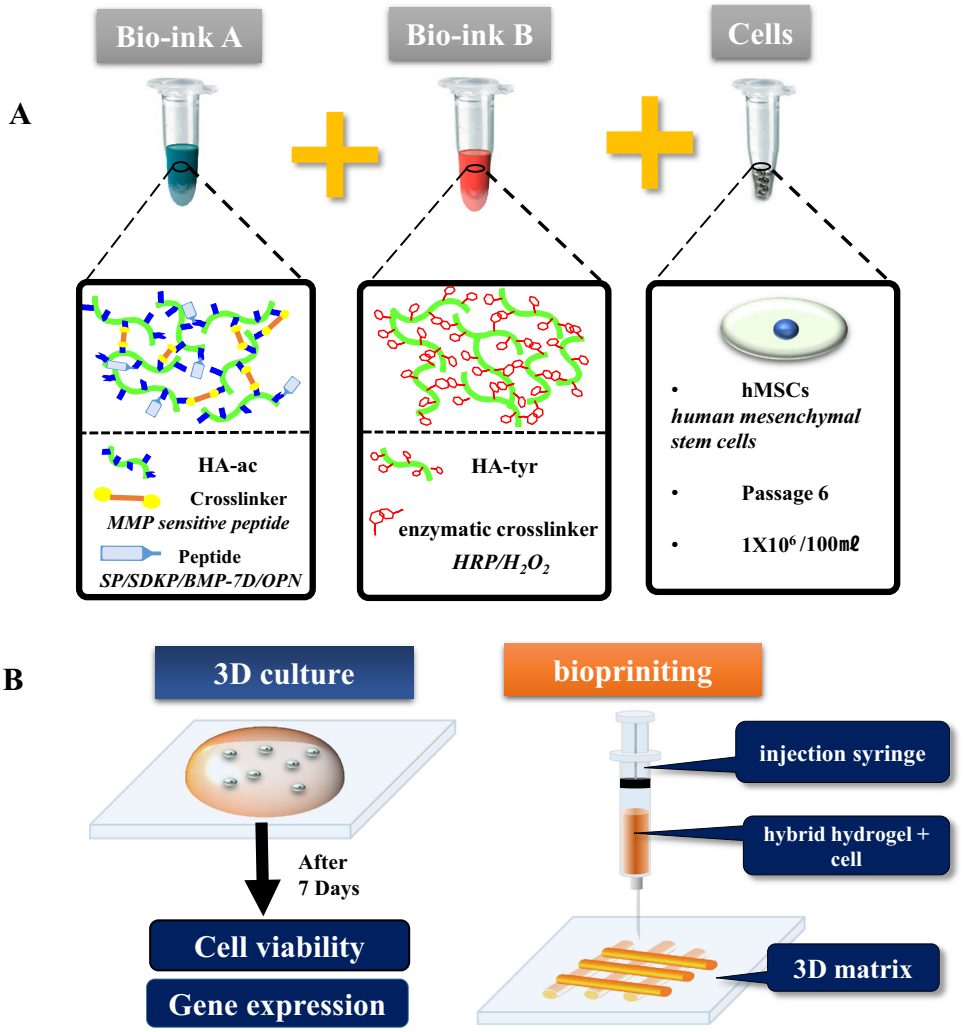

Fig. 1 Schematic diagram illustrating the hyaluronic acid-based hybrid bio-ink. **A** Representations of hybrid bio-ink formation. Bio-ink A: acrylated hyaluronic acid for immobilizing bioactive peptide. Bio-ink B: tyramine-conjugated hyaluronic acids for fast gelation. L929 cells or hMSC suspension was mixed with a Bio-ink A and Bio-ink B solution with peptides (1×10^6 cells/100 µl gel). **B** Overview of 3D culture and patterning process of hybrid bio-ink

3 Results and discussion

3.1 Hybrid bio-ink formation and characterization

Hyaluronic acid, one of the major components of extracellular matrix protein, was used as one of the basic building blocks of the bio-inks used for bioprinting [22]. A major challenge of bio-ink is integrating biological functions into mechanically integrated structures. Therefore, we synthesized and prepared dual function hydrogels, incorporating biological functions and mechanical integrity, based on hyaluronic acid (Fig. 1). For biological functions guiding mesenchymal stem cell differentiation, biofunctional peptides containing a SH-group in the N-terminal of peptides were immobilized via Michael type addition reaction to the acrylated hyaluronic acids, as in the previous study [23]. Acrylated HA was produced by a two-step reaction using ADH and NAS Michael type addition reaction, which allowed the immobilization of cysteine containing bioactive peptides on the hydrogel. Matrix metalloprotease sensitive peptides were used as crosslinkers for controlling remodeling rates of the hydrogel [24]. To achieve structural integrity, hyaluronic acid was derivatized using tyramine. HA–Tyr conjugate was synthesized by amide bond formation between the amine group of tyramine and the carboxyl group of HA after activation with EDC and sulfo-NHS. H-NMR confirmed the successful synthesis of HA-tyr conjugation (Fig. S1). HA-Tyr conjugates were crosslinked through the enzyme-mediated coupling of tyramine moieties by H_2O_2 and HRP, as described in the previous study [21].

Gelation kinetics of the novel hybrid hydrogel was important in the application of bio-inks. Kinetics measured via rheometer showed a gelation time of less than 200 s, which is sufficient for constructing structures using a bio-ink (Fig. 2A). For the gelation velocity of bio-ink, bio-ink with a long gelation time is difficult to pattern quickly because of difficulty in maintaining the form of the pattern. Thereby, the short gelation time of bio-ink is needed to form the desired structure and to increase the survival rate

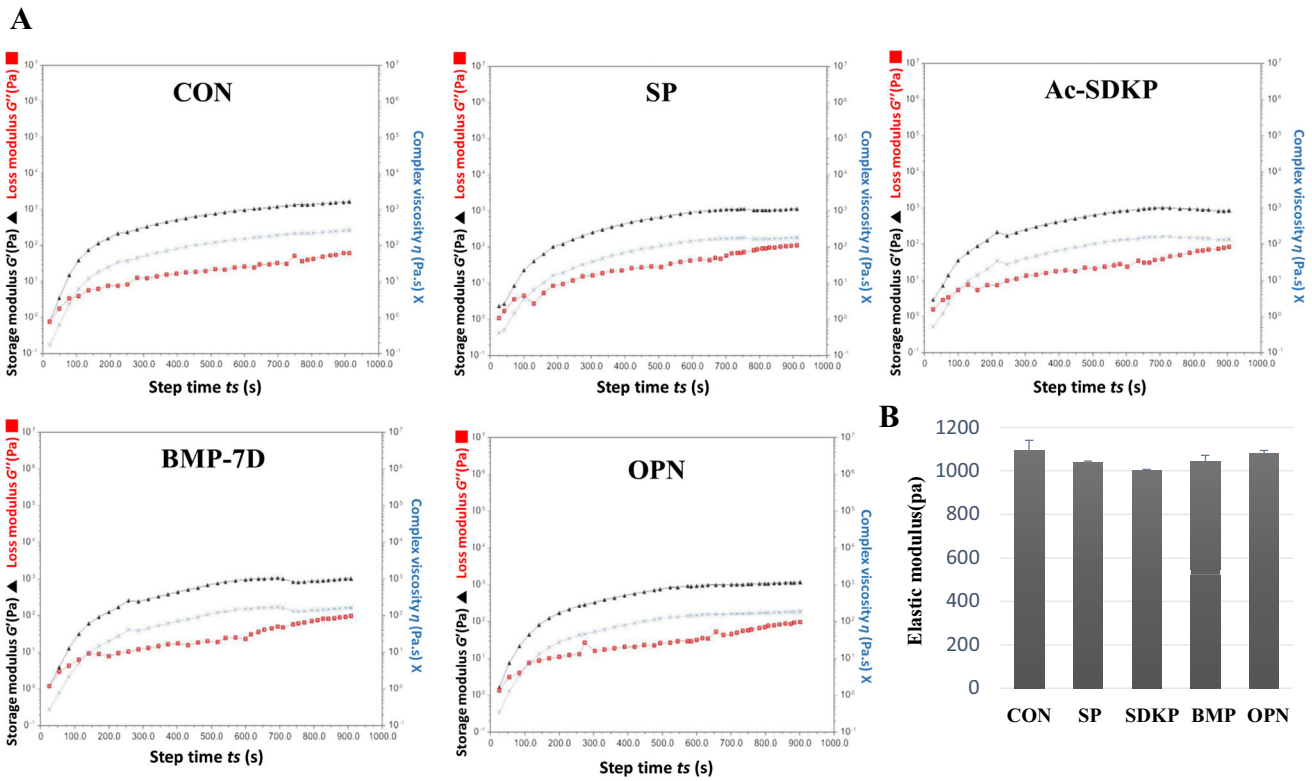

Fig. 2 Comparison of mechanical properties of peptide-hybrid bio-ink. **A** Gelation kinetics of peptides-hybrid bio-ink. Typical evolution of the storage modulus G′ (filled triangle), loss modulus G″ (filled square) and complex viscosity η^* (X) of hybrid multi-functional bio-ink. **B** Elastic modulus during frequency sweep of peptides-hybrid multi-functional bio-ink. The measurement was taken with constant deformation of 1% at 1 Hz and 37 °C

of the encapsulated cells. Where, maintaining the shape of the desired structure is related to the interconnectivity of the pores. In particular, the used 3D printing technology has advantages that guarantee interconnected pores of scaffold. Adequate pores during implantation are reported that has been favorable for the nutrient supply and metabolic waste removal in the scaffold [25]. Therefore, it can be explained that the bio-ink with short gelation time has the effect of maintaining the pore shape, and it can help the biological functions of scaffold. Hydrogels with various types of cross-linkers and biopeptides, such as SP, SDKP, BMP-7D, and OPN peptides, showed similar gelation kinetics, reflecting that the incorporation of bioactive peptides does not change the physical properties of the hydrogel (Fig. 2B). The ratio of acrylated HA and tyramine-conjugated HA was set to 9–1 to attain mechanical integrity up to 1 kPa. In our previous study, acrylated HA-based hydrogels with 1 kPa showed higher proliferative activity among mesenchymal stem cells [26]. Based on those results, novel hybrid hydrogels with tyramine could get have benefits of fast gelation and active cell proliferation.

3.2 Viability of L929 cells in hybrid hydrogels

Higher cell viability in the hydrogel is an essential requirement of bio-ink. Because the gelation process includes enzymatic reactions, chemical addition reactions and highly reactive chemicals, such as hydrogel peroxide, these reactions could affect the viability of the cells in the hydrogel. We optimized the reactions by varying the concentration of hydrogen peroxide and horseradish peroxidase. A higher concentration of hydrogen peroxide (> 0.6 mM) led to lower survival rates in cells assayed by live/dead cell assay kits, although it had a faster gelation time (Fig. S2). Our results indicate that cell viability in the hydrogel was 90% after culturing in the hydrogel for 7 days (Fig. 3). Interestingly, cells in the hydrogel remained round instead of spreading in the 3D matrix, even though cells in the gel were still alive, a common phenomenon of *in vitro* cell culture in hydrogel [27]. Although cells did not change their morphology in the 3D hydrogel, cells started differentiation depending on the composition of hydrogel immobilized with different bioactive peptides.

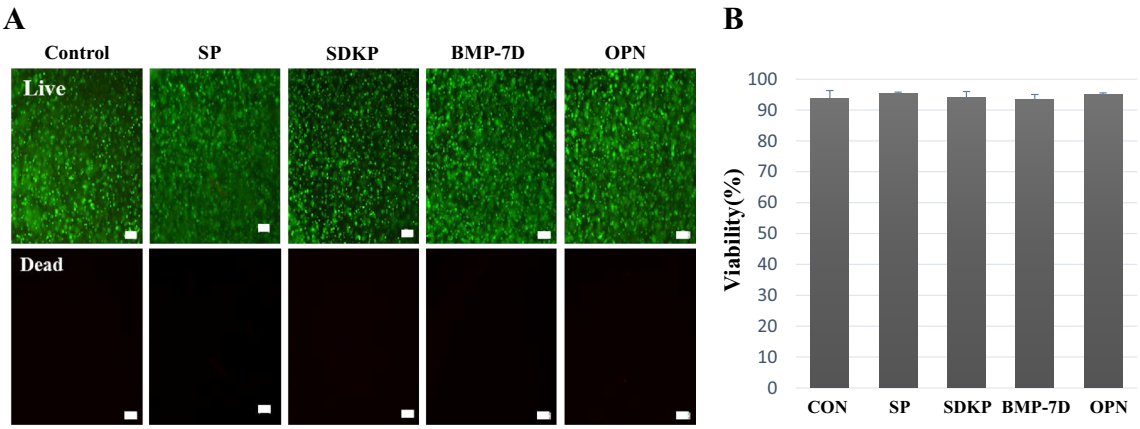

Fig. 3 Viability of L929 cells in the hybrid multi-functional bio-ink by live and dead assay. **A** Photographs and **B** comparison of viability of L929 cells in the hybrid multi-functional bio-ink. L929 cells were cultured for 7 days in hybrid multi-functional bio-ink. The membranes of live cells were labeled green fluorescence and the nuclei of dead cells with red (n= 6). Scale bars: 100 μm

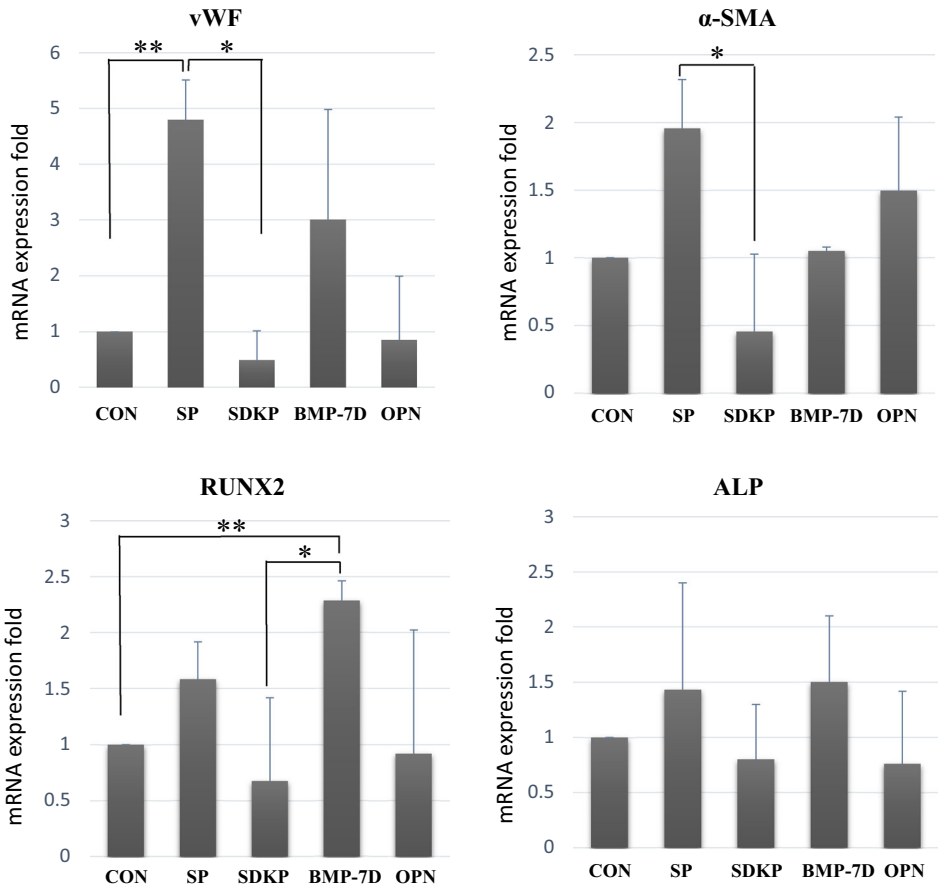

Fig. 4 Gene expression of hMSCs in various peptide-hybrid bio-inks by real-time PCR at 7 days. mRNA expression levels of von Willebrand factor (vWF), smooth muscle actin (α-aSMA), RUNX2 and ALP were significantly higher in the SP and BMP-7D group than in the control, SDKP, or OPN groups. $^{*}p < 0.05$; $^{**}p < 0.01$

3.3 Evaluation of angiogenic and osteogenic differentiation in hybrid hydrogel with peptides

Stem cells have two unique characteristics, self-renewal and differentiation. For bioprinting research, guiding stem cells into terminally differentiated cells is a major concern [28]. Various cocktails for guiding stem cell differentiation have been elucidated, including growth factors, peptides, and chemicals. We immobilized bioactive peptides to add guidance signals in the bio-ink [29–31]. Because angiogenesis and osteogenesis are major events in bone regeneration, we used peptides to induce angiogenesis and

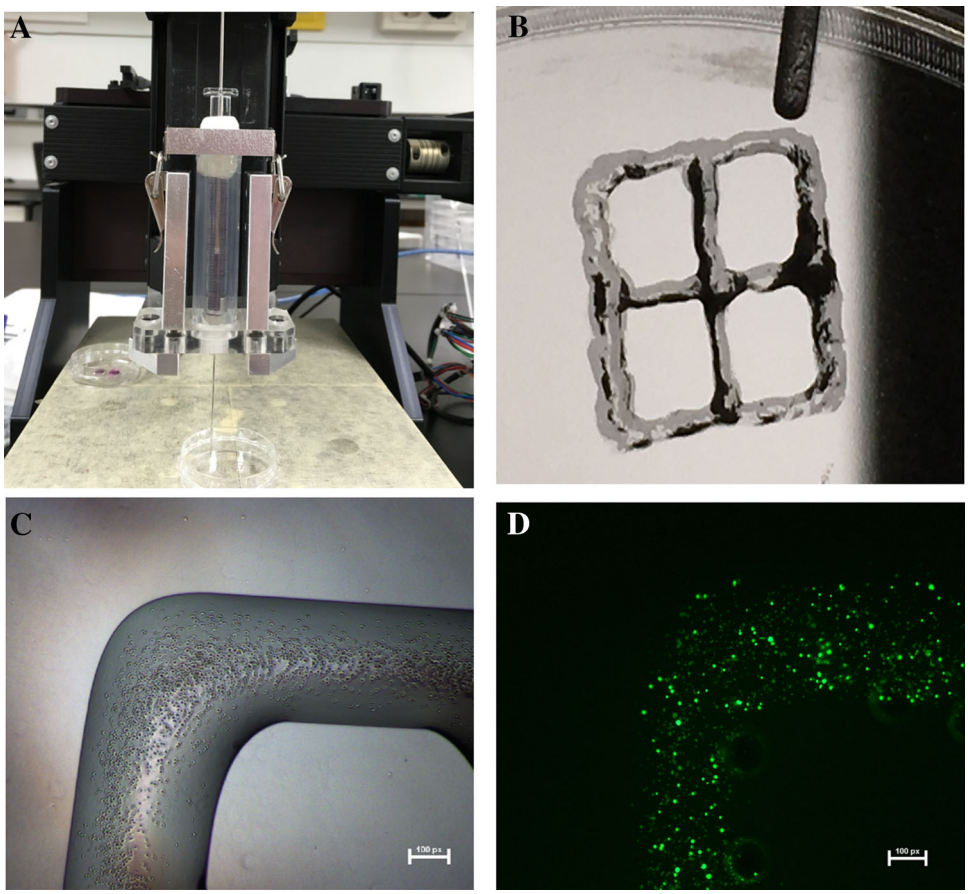

Fig. 5 Bioprinting of 3D grid pattern structure. **A** Lab-made 3D printer. **B** The width (W) and distance (D) were both 5 mm at the fabricated simple-grid scaffold. **C** Cell-encapsulated hydrogel scaffold with simple grid was fabricated using a needle with an inner diameter of 150 μm. **D** Cell viability assay showed that cells were alive in the bio-printed hydrogel. Scale bars: 100 μm

osteogenesis in the hybrid hydrogel. For angiogenesis, we used SDKP [18], a derived thymosin beta known as a potent angiogenic agent, and SP, a neuroangiogenic peptide [32]. For osteogenesis, we used a BMP-7D, known as a potent moderator [33], and OPN, known as bone-forming factors [34]. Immobilization of four different peptides demonstrated the differential angiogenic and osteogenic effects on the stem cells (Fig. 4).

The SP immobilized groups expressed significantly higher endothelial-specific markers (vWF) compared with the control group. The smooth muscle cell marker (α-SMA), which is indicative of the mature vessels, was also higher expressed about two times higher than the control group. Previous studies have shown that SP causes angiogenesis through the differentiation or recruitment of hMSCs [35–37]. Our results suggest that hydrogel immobilized SP affects the EC and muscle cell differentiation of hMSCs. In addition, osteogenic genes (RUNX2 and ALP) were also increased in hybrid hydrogels with immobilized SP compared to the control. SP has been demonstrated to contribute to bone growth by stimulating the proliferation and differentiation of stem cells [38]. SP binds to the NK1 receptor and activates the Wnt/β-catenin signaling pathway in BMSCs [39, 40]. The Wnt/β-catenin signaling pathway was proposed as an upstream activator of BMP2 expression [41]. It also affects the expression of RUNX2, a master transcription factor that regulates bone formation, and BMSCs can differentiate into osteoblasts with increased osteocalcin and alkaline phosphatase activity [42].

Our gene expression results found that BMP-7D induced the highest osteogenic differentiation, as well as angiogenic differentiation of stem cells. BMP-7D is a member of the bone morphogenetic protein family. SMAD-dependent-BMP signaling binds to receptors (RI, RII) and then signals are transduced to the SMAD. Activated SMADs regulate expression of the master transcription factor regulating bone formation transcriptional factors (RUNX2) and promote osteogenic genes such as ALP [43], which was correlated with our RT-PCR results. BMP-7 peptide transduced muscle-derived progenitor cells differentiated into osteoblasts, as assessed by ALP activity [44]. It is also known that BMP-7 increased VEGF expression for angiogenesis [45]. These results indicate that BMP-7D immobilized hydrogels could increase osteogenesis as well as angiogenesis.

In the hybrid bio-ink immobilized OPN, α-SMA was 1.5 times higher than control, which agrees with the reports that OPN regulates the migration and proliferation of α-

SMA [46–48]. However, it has been shown that OPN is not effective in differentiation into osteoblast in our hybrid hydrogel. SDKP also did not affect the angiogenic and osteogenic effect. Based on the results, it can be expected that bone regeneration and angiogenesis can be expected at the same time when hybrid hydrogel with immobilized SP and BMP-7D is used as bio-ink.

3.4 Preparation of hMSC-laden bio-ink, fabrication of constructs, and viability

For the assessment of the feasibility of hydrogels as a bio-ink, we tested the printability of the bio-ink using a microextrusion bioprinter and assessed cell viability after printing. Hybrid hydrogel solution was mixed with stem cells in a Hamilton syringe and injected onto glass slides for printing structures (Fig. 5A). Due to the higher viscosity of the hydrogel, we could successfully print multiple grid shapes (Fig. 5B). Printed hydrogels maintained their mechanical integrity after printing and encapsulated stem cells in the hydrogel (Fig. 5C). Cell viability assay 1 day after bioprinting found that cells in hydrogel showed higher viability (> 90%; Fig. 5D). This result indicates that our novel hybrid bio-ink can be used as a bio-ink for patterning structures of cells and ECMs. Further study is required for layer-by-layer assembly of hydrogels using 3D patterning in tissue engineering.

Acknowledgement This study was supported by a grant from the Ministry of Health and Welfare in the Republic of Korea (HI14C2143).

Compliance with ethical standards

Conflict of interest The authors have no financial conflict of interest.

Ethical Statement There are no animal experiments carried out for this article.

References

1. Ozbolat IT, Yu Y. Bioprinting toward organ fabrication: challenges and future trends. IEEE Trans Biomed Eng. 2013;60:691–9.
2. Kim JH, Yoo JJ, Lee SJ. Three-dimensional cell-based bioprinting for soft tissue regeneration. Tissue Eng Regen Med. 2016;13:647–62.
3. Park JH, Jang JA, Lee JS, Cho DW. Current advances in three-dimensional tissue/organ printing. Tissue Eng Regen Med. 2016;13:612–21.
4. Murphy SV, Atala A. 3D bioprinting of tissues and organs. Nat Biotechnol. 2014;32:773–85.
5. Murphy SV, Skardal A, Atala A. Evaluation of hydrogels for bioprinting applications. J Biomed Mater Res A. 2013;101:272–84.
6. Seol YJ, Kang HW, Lee SJ, Atala A, Yoo JJ. Bioprinting technology and its applications. Eur J Cardiothorac Surg. 2014;46:342–8.
7. Malda J, Visser J, Melchels FP, Jüngst T, Hennink WE, Dhert WJ, et al. 25th anniversary article: engineering hydrogels for biofabrication. Adv Mater. 2013;25:5011–28.
8. Kim JE, Kim SH, Jung YM. Current status of three-dimensional printing inks for soft tissue regeneration. Tissue Eng Regen Med. 2016;13:636–46.
9. Stanton MM, Samitier J, Sánchez S. Bioprinting of 3D hydrogels. Lab Chip. 2015;15:3111–5.
10. Colosi C, Shin SR, Manoharan V, Massa S, Costantini M, Barbetta A, et al. Microfluidic bioprinting of heterogeneous 3D tissue constructs using low-viscosity bioink. Adv Mater. 2016;28:677–84.
11. Li C, Faulkner-Jones A, Dun AR, Jin J, Chen P, Xing Y, et al. Rapid formation of a supramolecular polypeptide-DNA hydrogel for in situ three-dimensional multilayer bioprinting. Angew Chem Int Ed Engl. 2015;54:3957–61.
12. Rutz AL, Hyland KE, Jakus AE, Burghardt WR, Shah RN. A multimaterial bioink method for 3D printing tunable, cell-compatible hydrogels. Adv Mater. 2015;27:1607–14.
13. Duan B, Hockaday LA, Kang KH, Butcher JT. 3D bioprinting of heterogeneous aortic valve conduits with alginate/gelatin hydrogels. J Biomed Mater Res A. 2013;101:1255–64.
14. Duan B, Kapetanovic E, Hockaday LA, Butcher JT. Three-dimensional printed trileaflet valve conduits using biological hydrogels and human valve interstitial cells. Acta Biomater. 2014;10:1836–46.
15. Pati F, Jang J, Ha DH, Won Kim S, Rhie JW, Shim JH, et al. Printing three-dimensional tissue analogues with decellularized extracellular matrix bioink. Nat Commun. 2014;5:3935.
16. Das S, Pati F, Choi YJ, Rijal G, Shim JH, Kim SW, et al. Bioprintable, cell-laden silk fibroin-gelatin hydrogel supporting multilineage differentiation of stem cells for fabrication of three-dimensional tissue constructs. Acta Biomater. 2015;11:233–46.
17. Benoit DS, Schwartz MP, Durney AR, Anseth KS. Small functional groups for controlled differentiation of hydrogel-encapsulated human mesenchymal stem cells. Nat Mater. 2008;7:816–23.
18. Song M, Jang H, Lee J, Kim JH, Kim SH, Sun K, et al. Regeneration of chronic myocardial infarction by injectable hydrogels containing stem cell homing factor SDF-1 and angiogenic peptide Ac-SDKP. Biomaterials. 2014;35:2436–45.
19. Kim J, Kim IS, Cho TH, Lee KB, Hwang SJ, Tae G, et al. Bone regeneration using hyaluronic acid-based hydrogel with bone morphogenic protein-2 and human mesenchymal stem cells. Biomaterials. 2007;28:1830–7.
20. Kuo YC, Chang YH. Differentiation of induced pluripotent stem cells toward neurons in hydrogel biomaterials. Colloids Surf B Biointerfaces. 2013;102:405–11.
21. Lee F, Chung JE, Kurisawa M. An injectable hyaluronic acid-tyramine hydrogel system for protein delivery. J Control Release. 2009;134:186–93.
22. Burdick JA, Prestwich GD. Hyaluronic acid hydrogels for biomedical applications. Adv Mater. 2011;23:H41–56.
23. Zhu J. Bioactive modification of poly(ethylene glycol) hydrogels for tissue engineering. Biomaterials. 2010;31:4639–56.
24. Kim J, Kim IS, Cho TH, Kim HC, Yoon SJ, Choi J, et al. In vivo evaluation of mmp sensitive high-molecular weight ha-based hydrogels for bone tissue engineering. J Biomed Mater Res A. 2010;95:673–81.
25. Oh SH, Park IK, Kim JM, Lee JH. In vitro and in vivo characteristics of PCL scaffolds with pore size gradient fabricated by a centrifugation method. Biomaterials. 2007;28:1664–71.
26. Kim J, Park Y, Tae G, Lee KB, Hwang SJ, Kim IS, et al. Synthesis and characterization of matrix metalloprotease sensitive-

low molecular weight hyaluronic acid based hydrogels. J Mater Sci Mater Med. 2008;19:3311–8.
27. Billiet T, Gevaert E, De Schryver T, Cornelissen M, Dubruel P. The 3D printing of gelatin methacrylamide cell-laden tissue-engineered constructs with high cell viability. Biomaterials. 2014;35:49–62.
28. Tasoglu S, Demirci U. Bioprinting for stem cell research. Trends Biotechnol. 2013;31:10–9.
29. Shi Y, Do JT, Desponts C, Hahm HS, Schöler HR, Ding S. A combined chemical and genetic approach for the generation of induced pluripotent stem cells. Cell Stem Cell. 2008;2:525–8.
30. Re'em T, Tsur-Gang O, Cohen S. The effect of immobilized RGD peptide in macroporous alginate scaffolds on TGFbeta1-induced chondrogenesis of human mesenchymal stem cells. Biomaterials. 2010;31:6746–55.
31. Takahashi T, Lord B, Schulze PC, Fryer RM, Sarang SS, Gullans SR, et al. Ascorbic acid enhances differentiation of embryonic stem cells into cardiac myocytes. Circulation. 2003;107:1912–6.
32. Kim JH, Jung Y, Kim BS, Kim SH. Stem cell recruitment and angiogenesis of neuropeptide substance p coupled with self-assembling peptide nanofiber in a mouse hind limb ischemia model. Biomaterials. 2013;34:1657–68.
33. Beederman M, Lamplot JD, Nan G, Wang J, Liu X, Yin L, et al. BMP signaling in mesenchymal stem cell differentiation and bone formation. J Biomed Sci Eng. 2013;6:32–52.
34. Standal T, Borset M, Sundan A. Role of osteopontin in adhesion, migration, cell survival and bone remodeling. Exp Oncol. 2004;26:179–84.
35. Ziche M, Morbidelli L, Pacini M, Geppetti P, Alessandri G, Maggi CA. Substance P stimulates neovascularization in vivo and proliferation of cultured endothelial cells. Microvasc Res. 1990;40:264–78.
36. Kohara H, Tajima S, Yamamoto M, Tabata Y. Angiogenesis induced by controlled release of neuropeptide substance P. Biomaterials. 2010;31:8617–25.
37. Um JH, Yu JY, Dubon MJ, Park KS. Substance P and thiorphan synergically enhance angiogenesis in wound healing. Tissue Eng Regen Med. 2016;13:149–54.
38. Shih C, Bernard GW. Neurogenic substance p stimulates osteogenesis in vitro. Peptides. 1997;18:323–6.
39. Wang L, Zhao R, Shi X, Wei T, Halloran BP, Clark DJ, et al. Substance P stimulates bone marrow stromal cell osteogenic activity, osteoclast differentiation, and resorption activity in vitro. Bone. 2009;45:309–20.
40. Mei G, Xia L, Zhou J, Zhang Y, Tuo Y, Fu S, et al. Neuropeptide SP activates the WNT signal transduction pathway and enhances the proliferation of bone marrow stromal stem cells. Cell Biol Int. 2013;37:1225–32.
41. Zhang R, Oyajobi BO, Harris SE, Chen D, Tsao C, Deng HW, et al. Wnt/β-catenin signaling activates bone morphogenetic protein 2 expression in osteoblasts. Bone. 2013;52:145–56.
42. Fu S, Mei G, Wang Z, Zou ZL, Liu S, Pei GX, et al. Neuropeptide substance P improves osteoblastic and angiogenic differentiation capacity of bone marrow stem cells in vitro. Biomed Res Int. 2014;2014:596023.
43. Chen G, Deng C, Li YP. TGF-β and BMP signaling in osteoblast differentiation and bone formation. Int J Biol Sci. 2012;8:272–88.
44. Franceschi RT, Wang D, Krebsbach PH, Rutherford RB. Gene therapy for bone formation: in vitro and in vivo osteogenic activity of an adenovirus expressing BMP7. J Cell Biochem. 2000;78:476–86.
45. Akiyama I, Yoshino O, Osuga Y, Shi J, Harada M, Koga K, et al. Bone morphogenetic protein 7 increased vascular endothelial growth factor (VEGF)-a expression in human granulosa cells and VEGF receptor expression in endothelial cells. Reprod Sci. 2014;21:477–82.
46. Yue TL, McKenna PJ, Ohlstein EH, Farach-Carson MC, Butler WT, Johanson K, et al. Osteopontin-stimulated vascular smooth muscle cell migration is mediated by beta 3 integrin. Exp Cell Res. 1994;214:459–64.
47. Weintraub AS, Schnapp LM, Lin X, Taubman MB. Osteopontin deficiency in rat vascular smooth muscle cells is associated with an inability to adhere to collagen and increased apoptosis. Lab Invest. 2000;80:1603–15.
48. Gao H, Steffen MC, Ramos KS. Osteopontin regulates alpha-smooth muscle actin and calponin in vascular smooth muscle cells. Cell Biol Int. 2012;36:155–61.